Signature of stripe pinning in optical conductivity

L. Benfatto and C. Morais Smith
Département de Physique, Université de Fribourg, Pérolles, CH-1700 Fribourg, Switzerland
(Received 25 June 2003; published 18 November 2003)

The response of charge stripes to an external electric field applied perpendicular to the stripe direction is studied within a diagrammatic approach for both weak and strong pinning by random impurities. The soundlike mode of the stripes described as elastic strings moves to finite frequency due to impurity pinning. By calculating the optical conductivity we determine this characteristic energy scale for both a single stripe and an array of interacting stripes. The results explain the anomalous far-infrared peak observed recently in optical-conductivity measurements on cuprates.

DOI: 10.1103/PhysRevB.68.184513 PACS number(s): 74.20.Mn, 74.25.Gz, 74.72.Dn

Recent optical conductivity measurements in high-T_c cuprates have revealed the existence of a strong peak in the far-infrared regime, which has been attributed to the presence of charge stripes.[1,2] The typical energy of this peak is much lower than the midinfrared band detected in previous experiments[3] and reproduced by numerical simulations of the Hubbard model.[4] A similar feature reported for slightly overdoped $Bi_2Sr_2CuO_6$ (Ref. 5) was explained in terms of a charge-ordering instability of the Fermi liquid.[6] However, these arguments cannot be extended to the underdoped regime, where the Fermi-liquid description breaks down and the charge degrees of freedom are known to order.[7]

In this paper we propose that this anomalous peak may originate from the pinning of the zero-energy phononlike mode associated with transverse fluctuations of stripes, which shifts to finite energies in the presence of impurities. We calculate the optical conductivity of striped systems using a diagrammatic approach, which allows us to determine the peak frequency for both weak and strong impurity pinning. In the single-stripe case, we find a peak at a frequency ν given by the ratio between the stripe velocity v and a characteristic impurity length scale λ, which is determined by the strength of the pinning. For a stripe array, a second energy scale ω_U, proportional to the strength U of the stripe-stripe interaction, becomes relevant. In the weak-pinning regime, which is appropriate for describing cuprates, a second peak appears around ω_U. When $\omega_U \sim \nu$, a resonance arises and the main peak splits. Our calculations yield a good estimate for the peak frequency measured in La cuprates[1,2,8] and clarify some peculiar features observed in experiments, such as the peaksharpening[1] and splitting[2] which occur when stripe-stripe interactions are important.

We begin by considering a single line of holes (stripe) embedded in a two-dimensional $l \times L$ antiferromagnetic background with lattice constant a. The transversal dimension l correspond to the interstripe distance when the stripe array is explicitly considered (see below). The stripe is oriented along the y axis and acts as a domain wall for the underlying magnetization. The holes are assumed to move in the transverse x direction and their dynamics is governed by the t-J model. In the long-wavelength limit a wavelike action describes the transverse displacement $u(y)$ of the stripe with respect to the equilibrium position.[9] The stripe velocity $v = \sqrt{Jta}$ is related to the kinetic energy of the holes (t) and the staggered magnetization (J) of the surrounding regions. In terms of the dimensionless displacement field $\psi = u/a$, the action reads

$$\mathcal{S} = \frac{1}{2at} \int d\tau dy [\mathcal{L}_0[\psi] + V[\psi]], \tag{1}$$

where $\mathcal{L}_0[\psi] = (\partial\psi/\partial\tau)^2 + v^2(\partial\psi/\partial y)^2$ and $V[\psi]$ is the pinning potential. In analogy with the standard problem of pinning of elastic manifolds,[10–12] the interaction of the (striped) density of carriers $\rho(\mathbf{r})$ with the short-range disorder potential $U(\mathbf{r}) = U_0 \Sigma_i \delta(\mathbf{r} - \mathbf{r}_i)$ can be written as $\int d\mathbf{r} U(\mathbf{r}) \rho(\mathbf{r}) \sim \rho_0 U_0 \Sigma_i \cos[2\pi(u - x_i)/l]$, where $\mathbf{r}_i = (x_i, y_i)$ denotes the position of the defects and ρ_0 is the average stripe density.[10] We consider that only defects localized near the stripe effectively act to pin it, so that the cosine term can be expanded around the minimum to yield, within the quadratic approximation $V[\psi] = V_0 at \Sigma_i [\psi(y) - \beta_i]^2 \delta(y - y_i)$. The impurities pin the local displacement $\psi(y_i)$ at a value β_i, with positive strength V_0, and we assume $\hbar = k_B = 1$.

In the absence of dynamical fluctuations, the stripe accommodates the impurity potential by adopting a configuration $\psi_0(y)$, which is a solution of the static equation of motion. The full, time-dependent solution $\psi(y,\tau)$ is described as a fluctuation around the equilibrium configuration $\psi_0(y)$, i.e., $\psi(y,\tau) = \psi_0(y) + \phi(y,\tau)$. Introducing the Fourier transform $\phi(q,\omega_m)$ with respect to the momentum q and the Matsubara frequency $\omega_m = 2\pi m T$, the reciprocal-space action for the ϕ field becomes

$$\mathcal{S} = \frac{1}{2} \sum_{q,\omega_m} \mathcal{D}_0^{-1}(q,\omega_m) |\phi(q,\omega_m)|^2 + \frac{V_0}{2} \sum_{q,q',\omega_m} \phi^\dagger(q-q',\omega_m) \phi(q,\omega_m) S(q), \tag{2}$$

where $S(q) = (1/L)\Sigma_i e^{iqy_i}$ is the form factor, and $\mathcal{D}_0(q,\omega_m) = at(\omega_m^2 + v^2 q^2)^{-1}$ is the bare Green function.

An electric field applied in the x direction, perpendicular to the stripe, generates a current $J = \int dy e(\partial\psi/\partial t)$. The linear charge density of the stripe is denoted by e/a. From the Kubo formula for the optical conductivity[13] $\sigma(\omega)$

$=e^2 i\omega\mathcal{D}(q=0,i\omega_m\to\omega-i\delta)$ and by analytic continuation in the lower half-plane of the dressed Green function $\mathcal{D}(q,\omega_m)$ one finds

$$\mathrm{Re}\,\sigma(\omega)=-e^2\omega\,\mathrm{Im}\,\mathcal{D}(q=0,i\omega_m\to\omega-i\delta). \tag{3}$$

In the absence of impurities, $\mathcal{D}$ coincides with the bare Green function $\mathcal{D}_0$. Its replacement in Eq. (3) yields the expected response of a massless, soundlike mode $\mathrm{Re}\,\sigma(\omega)=e^2at\delta(\omega)$. The dressed Green function $\mathcal{D}$ may be evaluated from the Dyson equation $\mathcal{D}^{-1}(q,\omega_m)=\mathcal{D}_0^{-1}(q,\omega_m)-\Sigma=(\omega_m^2+v^2q^2-\Gamma t)/(at)$, where we have performed a rescaling $\Sigma=\Gamma/a$ such that Γ has dimensions of energy. The self-energy Γ is evaluated by averaging the product of several $S(q)$ factors, which appear in each term of the perturbative series for Γ, over the random impurity positions.[13] Crossing diagrams, arising from scattering processes by different impurities, correspond to increasing powers of the impurity density n_i. If Γ is evaluated up to order V_0^2, crossing terms do not appear (Born approximation) and one obtains

$$\Gamma(\omega_m)=-\frac{V_0}{2}n_ia+\left(\frac{V_0}{2}\right)^2 n_ia\frac{1}{L}\sum_q D_0(q,\omega_m), \tag{4}$$

where $\mathcal{D}_0$ was used for calculating the second-order correction. On defining the frequency $\omega_0=n_iv=n_ia\sqrt{Jt}$, the dimensionless quantities $\tilde{\omega}=\omega/\omega_0$, $G=\Gamma t/\omega_0^2$, and the parameter $\alpha=V_0/(2n_iaJ)$, Eq. (4) takes the form

$$G=-\alpha-\frac{i\alpha^2}{2\tilde{\omega}}. \tag{5}$$

According to Eq. (3) the optical conductivity is given by

$$\mathrm{Re}\,\sigma(\omega)=-\sigma_0\frac{\tilde{\omega}G''}{(\tilde{\omega}^2+G')^2+G''^2}, \tag{6}$$

where $\sigma_0=e^2at/\omega_0$ and $G=G'+iG''$. Note that as soon as a real part is generated in G, the delta function in the optical conductivity moves to a finite frequency and its amplitude is determined by G''. Using Eq. (5), we find

$$\mathrm{Re}\,\sigma(\omega)=\sigma_0\frac{2(\omega/\nu)^2}{4(\omega/\nu)^2[(\omega/\nu)^2-1]^2+\alpha}, \tag{7}$$

with $\nu=\sqrt{\alpha}\omega_0$. We note that $\mathrm{Re}\,\sigma(\omega)\to 0$ both as $\omega\to 0$ and as $\omega\to\infty$, and has a peak at $\omega\simeq\nu$, as shown by the solid line in Fig. 1(a). The parameter α, which controls the perturbative expansion for G, depends both on the ratio V_0/J, i.e., the competition between impurity potential and elastic energy, and on the number of impurities per site n_ia. Thus the weak-pinning limit, where only first powers of α need be considered [as in Eq. (5)], is realized for a large number $(n_ia\sim 1)$ of weak $(V_0/J\ll 1)$ impurity centers. In this case, Eq. (7) shows that the peak frequency scales according to $\nu\simeq\sqrt{V_0tn_ia}$, moving toward zero energy as the strength of the pinning potential decreases. In the evaluation of Eq. (4), we used the bare Green function $\mathcal{D}_0$. The divergence of the self-energy (5) at small ω indicates the break down of this crude approximation at low frequencies. Inclusion of the next-order term in the perturbative expansion shows that higher-order diagrams become important for $\omega<\sqrt{\alpha}\nu/2$, i.e., at frequencies much smaller than ν. It has been argued[11] that a better result for G may be achieved by using the dressed Green function in Eq. (5), which leads to the self-consistent equation $G=-\alpha+(\alpha^2/2)(-\tilde{\omega}^2-G)^{-1/2}$. However, the resulting expression for $\sigma(\omega)$ shows a spurious gap below $\omega\approx 0.7\nu$, which is thought to originate from the fact that the self-consistent Born approximation selects arbitrarily a subset of diagrams of higher order in α without including crossing terms, whose contribution cannot be excluded if n_ia is large. Because we are interested primarily in the evaluation of the peak frequency ν, and not on details of the low-frequency behavior of $\sigma(\omega)$,[14] we restrict our analysis to the non-self-consistent Born approximation, which provides a reliable estimate both of the maximum of $\sigma(\omega)$ and of its scaling with α.

A different approach must be considered in the strong-coupling limit $\alpha\gg 1$, which corresponds to a small number $(n_ia\ll 1)$ of strong $(V_0/J\gg 1)$ pinning centers. In this case one might expect that the entire perturbative series in α should be resummed, but a criterion exists for selecting the relevant higher-order diagrams. For $n_ia\ll 1$, it is possible to select the subset of diagrams of first order in n_i after averaging over the impurity distribution (T-matrix approximation).[13] By explicit summation of the resulting series, using the full Green function $\mathcal{D}$ while evaluating each diagram, one obtains a self-consistent equation for G. In the limit $\alpha\to\infty$, one finds the analytical solution $\mathrm{Re}\,\sigma(\omega)=2\sigma_0\sqrt{\tilde{\omega}^2-1}/\tilde{\omega}^3$ for $\tilde{\omega}>1$ and $\mathrm{Re}\,\sigma(\omega)=0$ for $\tilde{\omega}<1$.[12] Thus, $\mathrm{Re}\,\sigma(\omega)$ displays a gap at ω_0 and a maximum at a frequency ω slightly above this value. When the solution is evaluated at arbitrary $\alpha\gg 1$, one finds essentially the same features. In this case the requirement of full self-consistency is crucial, and the gap feature arises from the strong pinning of the sound mode. The difference between the weak- and strong-pinning results can be understood by considering that in both cases the peak frequency corresponds to the sound mode of a free string, which is now trapped on a characteristic length scale λ. When few strong impurities are present, λ is given by the average distance between impurities $1/n_i$ and the peak appears at the frequency ω_0. However, when the number of impurities increases and V_0 decreases, the elastic energy cost of accommodating the string on a length scale $1/n_i$ is too high, and ψ is pinned on the Larking length λ_{loc}.[10,15] Dimensional estimates based on Eq. (1) yield $\lambda_{\mathrm{loc}}\sim v/\sqrt{V_0n_iat}$, which indeed corresponds to the characteristic frequency ν in the weak-pinning regime.

Until now we have concentrated on the transverse pinning of a single stripe. However, a more realistic description of cuprates requires the study of an array of stripes. By considering a harmonic coupling strength U between neighboring stripes, which are labeled by an index $n=1,\ldots,N$, we obtain the action[16]

$$S=\frac{1}{2at}\sum_n\int d\tau dy\{\mathcal{L}[\psi_n]+Ut(\psi_n-\psi_{n+1})^2+V[\psi_n]\}.$$

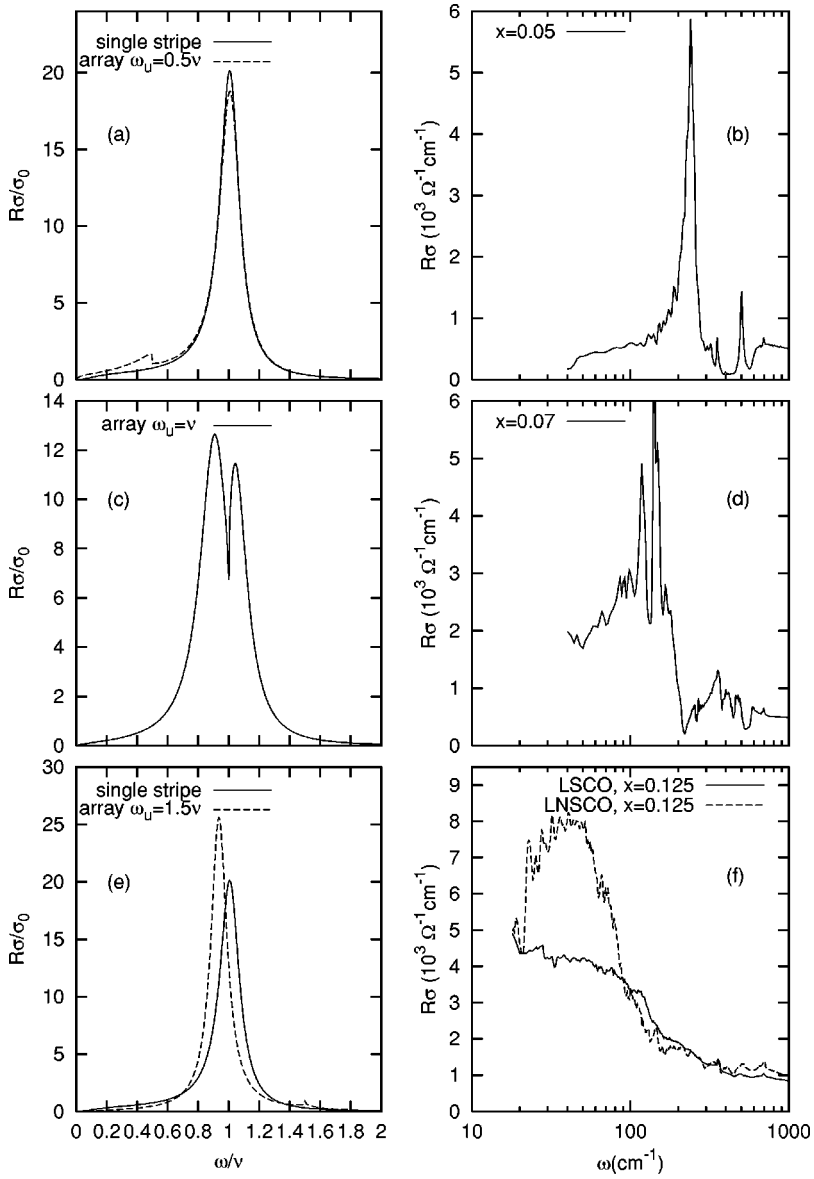

FIG. 1. Left: real part of the optical conductivity, in units of σ_0, as a function of ω/ν evaluated in the Born limit ($\alpha=0.1$). When interaction between stripes is not relevant [$\omega_U<\nu$ (a)] one finds a single peak (the second one for the stripe array is almost suppressed), as observed in LSCO at $x=0.05$ (b) (Ref. 2). When the resonance condition $\omega_U=\nu$ is satisfied, the peak at $\omega=\nu$ splits into two equally weighted peaks (c), as observed experimentally at $x=0.07$ (d) (Ref. 2). By increasing the interstripe interaction [$\omega_U=1.5\nu$ (e)] the peak sharpens and moves to slightly lower frequencies, as observed experimentally by comparing Nd-free with Nd-doped LSCO compounds (f) (Ref. 1). For comparison with our zero-temperature calculations, we display the experimental data at the lowest measured temperatures above T_c. Notice the logarithmic scale on the right panels.

Here $\psi_n=\psi_n(y,\tau)$ and the fluctuating field $\phi_n(y,\tau)\equiv\phi(x=nl,y,\tau)$ is a function of the discrete x values. By repeating the same steps as before, we observe that Eq. (2) is still valid, on taking $q\rightarrow\mathbf{q}=(q_x,q_y)$, $S(\mathbf{q})=(LN)^{-1}\Sigma_{ni}e^{iq_xnl+iq_yy_i^n}$, where y_i^n is the impurity coordinate at the nth stripe, and $\mathcal{D}_0$ becomes

$$\mathcal{D}_0(\mathbf{q},\omega_m)=\frac{at}{\omega_m^2+v^2q_y^2+4Ut\sin^2(q_xl/2)}. \tag{8}$$

The system of interacting stripes displays an anisotropic soundlike mode at long wavelengths, with an effective elastic coefficient U/a in the x direction, and an optical mode at $q_xl=\pi$ with energy $\omega_U=2\sqrt{Ut}$.

The general procedure used above to address the effect of disorder is extended readily to the case of interacting stripes. We assume that the average density of impurities does not depend on the stripe index n, i.e., $n_i^n=n_i$. In the Born limit, the main difference with respect to the single-stripe case arises from the additional integration in q_x of the Green function $\mathcal{D}_0$ in Eq. (4). By introducing the rescaled variables and $\overline{\omega}=\omega/\omega_U$, one obtains

$$G=-a+\frac{\alpha^2}{\pi}\frac{\omega_0}{\omega_U}\int_0^{\pi/2}dx\frac{1}{\sqrt{\sin^2x-\overline{\omega}^2}}. \tag{9}$$

When $\overline{\omega}>1$ the second term in Eq. (9) contributes only to G''. In the limit of vanishing stripe-stripe interaction $U\rightarrow 0$, or $\overline{\omega}\rightarrow\infty$, it reproduces the single-stripe result (5). For finite U, a second energy scale ω_U is relevant for determining the optical conductivity, which is defined by Eq. (3) with q replaced by $\mathbf{q}$. The additional feature is the divergence of G'' at ω_U, which leads to a second peak around this frequency, where $\mathrm{Re}\,\sigma(\omega)$ vanishes. The vanishing of the conductivity at ω_U in the weak-pinning regime should indeed be expected: at this energy, neighboring stripes fluctuate in antiphase, and because the total current arises from the sum of

the currents of each stripe, the net current in such a case is zero. At $\omega_U \ll \nu$ or $\omega_U \gg \nu$ the peak at ω_U is almost completely suppressed by the overall decrease of $\mathrm{Re}\,\sigma(\omega)$ at small and high frequencies, see dashed lines in Figs. 1(a) and 1(e). However, when $\omega_U \simeq \nu$ the peak at $\omega \simeq \nu$ splits [Fig. 1(c)], signaling a resonance between the characteristic mode of the stripe array at the zone boundary and the characteristic frequency of soundlike oscillation of each stripe at the Larkin length. Dimensional estimates indicate that this resonance arises when the average stripe separation coincides with the Larkin length. Moreover, for the stripe array we observe a sharpening of the peak for $\omega_U > \nu$ due to the flattening of G'' around ν [dashed line in Fig. 1(e)]. The softening of the peak frequency for $\omega_U > \nu$ scales according to $\alpha^2 \nu/\omega_U$, so it never moves far away from ν.

In the strong-pinning regime the qualitative behavior of $\mathrm{Re}\,\sigma(\omega)$ for the stripe array is similar to that of the single stripe, and no resonance is observed. Because the interaction with the impurities is the predominant effect, the behavior of G is almost entirely dominated by the pinning of the sound mode at ω_0. More details about the strong-pinning regime will be presented elsewhere.[17]

We next compare our results with the available experimental data. The velocity of the unpinned sound mode may be estimated by using standard values $t \sim J \sim 0.1$ eV for cuprates. The other relevant quantity is n_i. In these materials, the chemical-substituted dopants, whose two-dimensional density is x/a^2 (x being the doping), simultaneously provide charge carriers in the plane and act as pinning centers. As we explained at the beginning, we consider that on average the impurities within a range l contribute to pin each stripe, i.e., $n_i = xl/a^2$. Neutron diffraction measurements have shown that in the underdoped regime ($0.05 < x < 0.12$) of $La_{2-x}Sr_xCuO_4$ (LSCO) $l = a/2x$,[7] which yields $n_i a = 1/2$ and $\omega_0 \sim 0.05$ eV. Because $n_i a \sim 1$ corresponds to the weak-pinning regime, we expect that the peak frequency is given by $\nu = \sqrt{\alpha}\,\omega_0$ and thus is reduced with respect to the estimate of ω_0, in agreement with experimental data, see Figs. 1(b), 1(d), 1(f).[1,2] As shown in Figs. 1(b)–1(f), the peak frequency softens as x increases. Even though we also expect a general decreasing of ν due to a screening effect on V_0, a more quantitative comparison with experimental data would require the inclusion of lattice effects, which is beyond the scope of this paper.

Another interesting feature can be explained by our calculations: with increasing doping concentration, stripe-stripe interactions become more important and one should consider the stripe array. Our results predict that the peak splits when the average stripe separation l is of the order of the Larkin length, see Fig. 1(c). This splitting has been observed for $x = 0.05$ doped LSCO, a single peak appears [Fig. 1(b)] whereas for $x = 0.07$ the peak splits [Fig. 1(d)].[2] Although the value of α as a function of doping x is in general not known, we may nevertheless estimate the peak frequency where the splitting arises as $\nu = v/l = 0.014$ eV $= 113$ cm^{-1}, in excellent agreement with the measured value [Fig. 1(d)].[2] Our calculations also allow us to understand the results obtained by Dumm *et al.*[1] in Nd-doped LSCO [Fig. 1(f)]: the broad peak observed in LSCO (Ref. 1) moves to slightly lower frequency and becomes sharper in the Nd-doped compound, where the stripe array is ordered.[7] We have shown that when interstripe interactions increase, the peak becomes slightly softer, narrower, and more intense [Fig. 1(e)], as observed experimentally. Note that in Ref. 1 the feature seen in the Nd-free sample in Fig. 1(f) was interpreted as an anomalous large Drude peak. However, we claim that a stripe signature is still present in these data, even though a partial overlap with the single-particle response is possible. Indeed, resistivity data from Ref. 1 give $\sigma(0) \simeq 8 \times 10^3 \Omega^{-1}\,\mathrm{cm}^{-1}$, which is much larger than the value obtained by extrapolating the supposed Drude peak. Moreover, a peak at nearly the same frequency is also seen at $x = 0.12$ in Ref. 2.

In addition, our results provide the correct order of magnitude for the peak height. The one-dimensional optical-conductivity unit $\sigma_0 \equiv \sigma_0^{1D}$ converts into a three-dimensional one as $\sigma_0^{3D} = \sigma_0^{1D}/ld = (2e^2/\hbar)(t/\omega_0)(x/d)$, where d is the interlayer spacing. At $x = 0.07$, using $d \simeq 6$ Å, we estimate the maximum of $\sigma(\omega)$ to be of order $10^3 \Omega^{-1}\,\mathrm{cm}^{-1}$, as experimentally observed.[2]

Note that longitudinal transport, which is possible for half-filled stripes as in the cuprates, was neglected in our approach. However, the experimental observation of the same far-infrared peak in nickelates,[18] which exhibit filled stripes, supports our hypothesis that the anomalous peak in the far-infrared regime originates from transverse fluctuations. In fact, our results could be used also to describe the nickelates, but in this case the effective t and J parameters within a one-band model are not known.

In conclusion, we calculated the contribution from stripe pinning to the optical conductivity in cuprates within a diagrammatic approach accounting for the presence of randomly distributed impurities. We found a peak in the far-infrared range at a frequency which has the same order of magnitude as observed in the experiments. In addition, our results explain the splitting of the peak, as well as the narrowing and increased intensity, which arise when stripe-stripe interactions are relevant.

We acknowledge fruitful discussions with D. Baeriswyl, P. Calvani, S. Caprara, T. Giamarchi, J. Lorenzana, B. Normand, and J. Tranquada. We thank the authors of Refs. 1,2 for providing us with the experimental data. This work was supported by the Swiss NSF under Grant No. 620-62868.00.

[1] M. Dumm, D.N. Basov, S. Komiya, Y. Abe, and Y. Ando, Phys. Rev. Lett. **88**, 147003 (2002).

[2] A. Lucarelli, S. Lupi, M. Ortolani, P. Calvani, P. Maselli, M. Capizzi, P. Giura, H. Eisaki, N. Kikugawa, T. Fujita, M. Fujita, and K. Yamada, Phys. Rev. Lett. **90**, 037002 (2003).

[3] S. Uchida, T. Ido, H. Takagi, T. Arima, Y. Tokura, and S. Tajima, Phys. Rev. B **43**, 7942 (1991).

[4] J. Lorenzana and G. Seibold, Phys. Rev. Lett. **90**, 066404 (2003).

[5] S. Lupi, P. Calvani, M. Capizzi, and P. Roy, Phys. Rev. B **62**, 12 418 (2000).
[6] S. Caprara, C. Di Castro, S. Fratini, and M. Grilli, Phys. Rev. Lett. **88**, 147001 (2002).
[7] J.M. Tranquada, B.J. Sternlieb, J.D. Axe, Y. Nakamura, and S. Uchida, Nature (London) **375**, 561 (1995).
[8] R.P.S.M. Lobo, F. Gervais, and S.B. Oseroff, Europhys. Lett. **37**, 341 (1997).
[9] C. Morais Smith, Yu.A. Dimashko, N. Hasselmann, and A.O. Caldeira, Phys. Rev. B **58**, 453 (1998).
[10] See T. Giamarchi and E. Orignac, *Theoretical Methods for Strongly Correlated Electrons*, edited by D. Senechal *et al.* (Springer, New York, 2003), and references therein.
[11] H. Fukuyama, J. Phys. Soc. Jpn. **41**, 513 (1976).
[12] H. Fukuyama and P.A. Lee, Phys. Rev. B **17**, 535 (1978).
[13] G.D. Mahan, *Many-Particle Physics* (Kluwer Academic, New York, 2000).
[14] M.M. Fogler, Phys. Rev. Lett. **88**, 186402 (2002).
[15] A.I. Larkin and Y.N. Ovchinnikov, J. Low Temp. Phys. **34**, 409 (1979).
[16] N. Hasselmann, A.H. Castro Neto, C. Morais Smith, and Y. Dimashko, Phys. Rev. Lett. **82**, 2135 (1999).
[17] L. Benfatto and C. Morais Smith (unpublished).
[18] N. Poirot-Reveau, P. Odier, P. Simon, and F. Gervais, Phys. Rev. B **65**, 094503 (2002).